Supplement of Atmos. Chem. Phys., 21, 17759–17773, 2021
https://doi.org/10.5194/acp-21-17759-2021-supplement


Atmospheric Chemistry and Physics Open Access

*Supplement of*

# Synergetic effects of $NH_3$ and $NO_x$ on the production and optical absorption of secondary organic aerosol formation from toluene photooxidation

**Shijie Liu et al.**

*Correspondence to:* Gehui Wang (ghwang@geo.ecnu.edu.cn)

## S1 OH Concentration Calculation Process

The OH concentration was calculated based on the decay ratio of toluene concentrations and the known rate constant with respect to OH. The change of toluene concentration over time can be expressed as:

$$-\frac{d[toluene]}{dt} = K_{OH} \times [OH] \times [toluene] \quad \text{(RS1)}$$

Where, $K_{OH}$ is the reaction rates constant of OH radicals with toluene ($K_{OH}$=5.7× $10^{-12}$ $cm^3$ $molecule^{-1}$ $s^{-1}$). Assuming that the concentration of hydroxide did not change during the experiment, then we can get:

$$\ln(\frac{[toluene]_0}{[toluene]_t})/t = K_{OH} \times [OH] \quad \text{(RS2)}$$

Thus, plotting the variation curve of $\ln([toluene]_0/[toluene]_t)$ vs. time t showed as Fig.S1. The $\ln([toluene]_0/[toluene]_t)$ in Fig.1(b) was not a straight line. This is because the OH is consumed as the reaction goes on. The evolution of OH concentration at experiment conditions was shown in Fig.S2. The different experiment conditions in this study did not affect the OH concentration obviously. The highest OH concentration of 1.0 × $10^8$ molecule $cm^{-3}$ was observed at the beginning of the reaction. The average OH concentration over the entire reaction period is 5.9 × $10^7$ molecule $cm^{-3}$.

## S2 $OS_C$ calculation

In most previous studies, $OS_C$ was estimated from the O/C and H/C data (Liu et al., 2015; Chen et al., 2019; Chhabra et al., 2011; Docherty et al., 2018; Kroll et al., 2011). Because nitrogen content is significant enough to be considered in carbon oxidation state calculation of Exp.2 - 4 in our study, the $OS_C$ value used here was calculated based on the O/C, H/C and N/C ratio.

For Exp.2 with $NH_3$ presence, particulate nitrogen is almost certainly in the form of ammonium salt with nominal oxidation numbers of -3. Alternatively, average $OS_C$ in Exp. 2 was calculated using the equation of $OS_C$ = 2 O/C – H/C +3 N/C. For Exp.4, toluene SOA formed with NOx presence, particulate nitrogen is almost certainly in the form of organic nitrates (i.e., -$ONO_2$ with nominal oxidation numbers of +5) (Park et

al., 2017; Ruggeri et al., 2016). Alternatively, average $OS_C$ in Exp. 4 can also be simply calculated using the following equation of intensity-weighted mean O/C, H/C, and N/C: $OS_C = 2\ O/C - H/C - 5\ N/C$.

Both $NH_3$ and NOx was presence in Exp.3, we estimated the contribution of $NH_3$ and NOx to organic nitrogen based on N:C value in Exp. 2 and Exp. 4, respectively. Average $OS_C$ in Exp. 3 was calculated as: $OS_C = 2\ O/C - H/C + \sigma_{NH3} \times 3\ N/C - \sigma_{NOx} \times 5\ N/C$. Here, $\sigma_{NH3}$ is the contribution rate of $NH_3$ to total organic nitrogen in SOA, and $\sigma_{NOx}$ is the contribution rate of NOx to total organic nitrogen in SOA."

**S3 PMF results**

Positive matrix factorization (PMF) is a receptor model and multivariate factor analysis tool (Paatero and Tapper, 1994; Paatero, 1997). Recently, the PMF model was used to provide better separation of different organic components through high-resolution (HR) mass spectra data (Liu et al., 2014). This model was expressed as below:

$$x_{ij} = \Sigma_p g_{ip} f_{pj} + e_{ij}$$

where i and j refer to values of j species in i samples, respectively, p is the number of factors, and used a least-squares fitting process, minimizing a quality of fit parameter.

In our study, CU AMS PMF Execute Tool v 3.04A, which was developed by Ulbrich et al. (Ulbrich et al., 2009), was used for the PMF analysis. High-resolution ion fragments at m/z from 12-160 were used. We generated the organic data matrices and the corresponding error matrices from PIKA v 1.15D. Ions were classified and down-weighted according to the signal-to-noise ratios (SNR). 0.2<SNR<2 was classified as the weak ions and down-weighted by a factor of 2, SNR<0.2 was bad ions and removed from the analysis. Since $O^+$, $HO^+$, $H_2O^+$ and $CO^+$ are related proportionally only to $CO_2^+$ in the fragmentation table, the error values for each of these m/z were multiplied to avoid excessive weighting of $CO_2^+$. The data were analyzed using the PMF2 algorithm (Paatero et al., 2002) with f peak varying between -1 and 1.

A summary of the PMF results is presented in Fig. S1-S3. After an extensive evaluation of the mass spectral profiles and time series of different number of factors and the rotational forcing parameter, fPeak, the 2-factor solution with fPeak = 0 was chosen for toluene SOA. The OA components of the 2-factor solution solved under different fPeak values show very similar mass spectral patterns.

The direct comparisons of the mass spectra and time series of 3-factor solution are shown in Fig. S4. The 3-factor solution splits the High-nitrogen OA (Hi-NOA) into two components for which we cannot offer a physically meaningful interpretation. While the results of 2-factor solution are also used in the familiar chamber study(Chen et al., 2021; Chen et al., 2019). We therefore choose the 2-factor solution.

# Tables

**Table S1.** The content of $NO_3^-$ and $NH_4^+$ in the particle-phase for each experiment

| | $[NOx]_0$ (ppb) | $[NH_3]_0$ (ppb) | $[NO_3^-]$/[Org] (%) | $[NH_4^+]$/[Org] (%) |
|---|---|---|---|---|
| Exp.2 | - | ~200 | - | 1.9 |
| Exp.3 | 62 | ~200 | 4.0 | 2.6 |
| Exp.4 | 63 | - | ＜0.2 | - |

# Figures

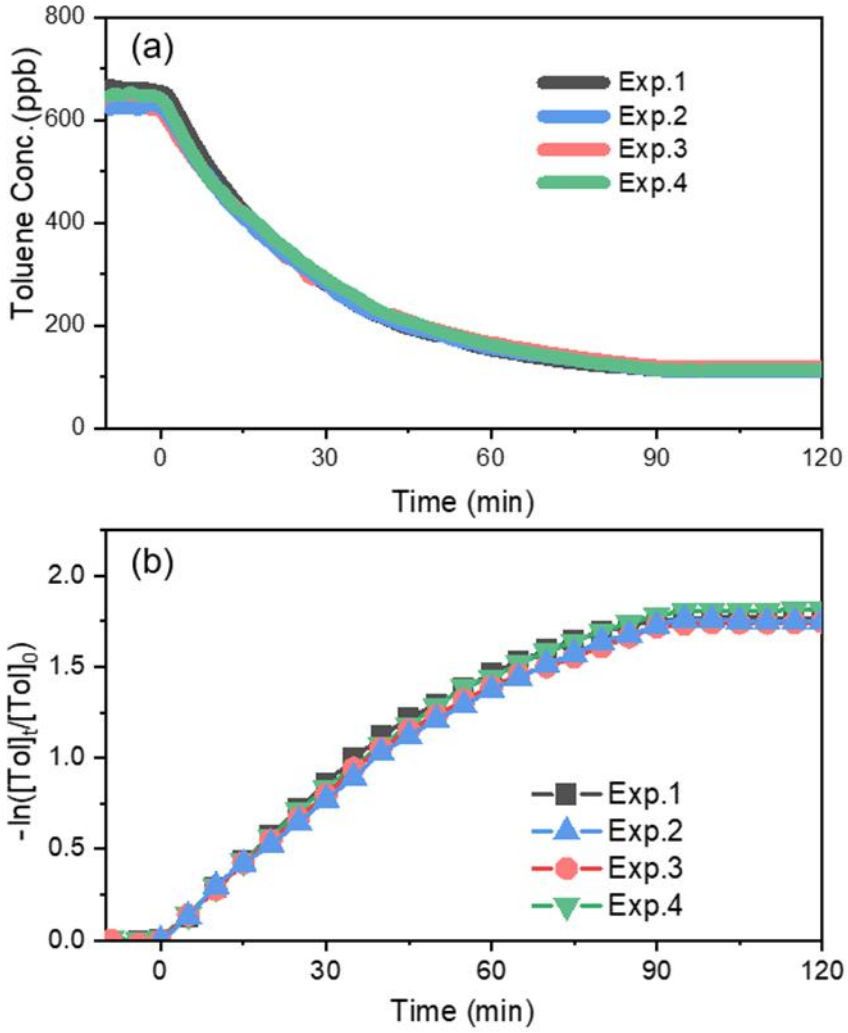


Fig. S1 The evolution of toluene concentration for each experiment.

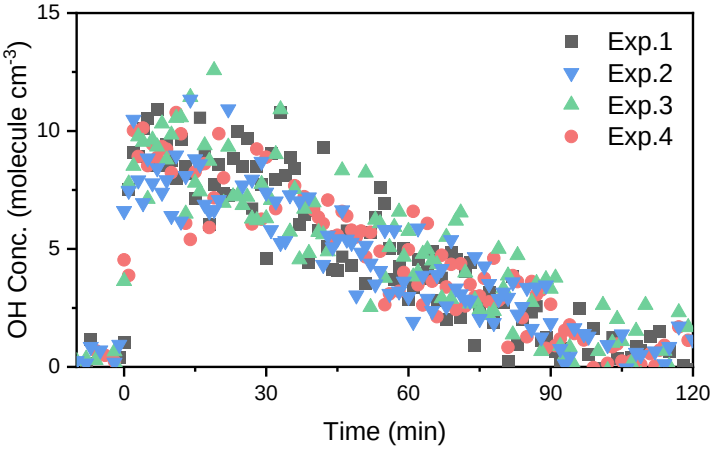


Fig. S2 The evolution of OH concentrations at different experiment conditions

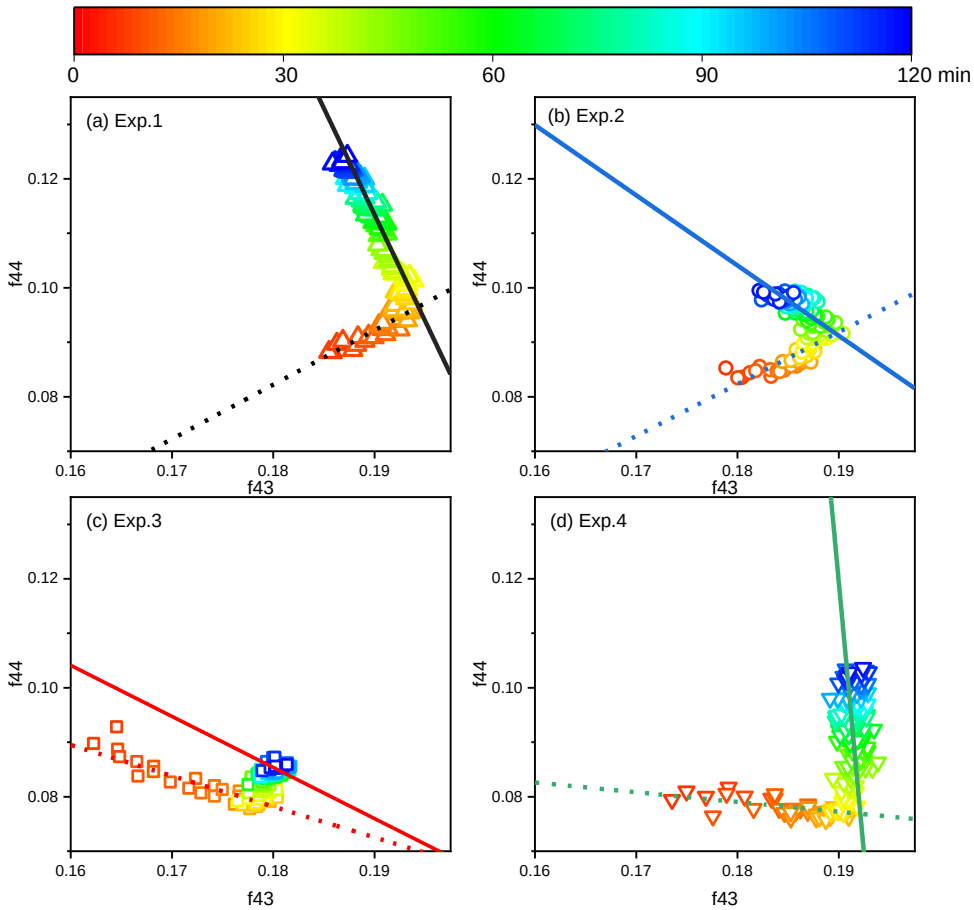


Fig. S4 Time-profile of f43 vs. f44 for different experiments

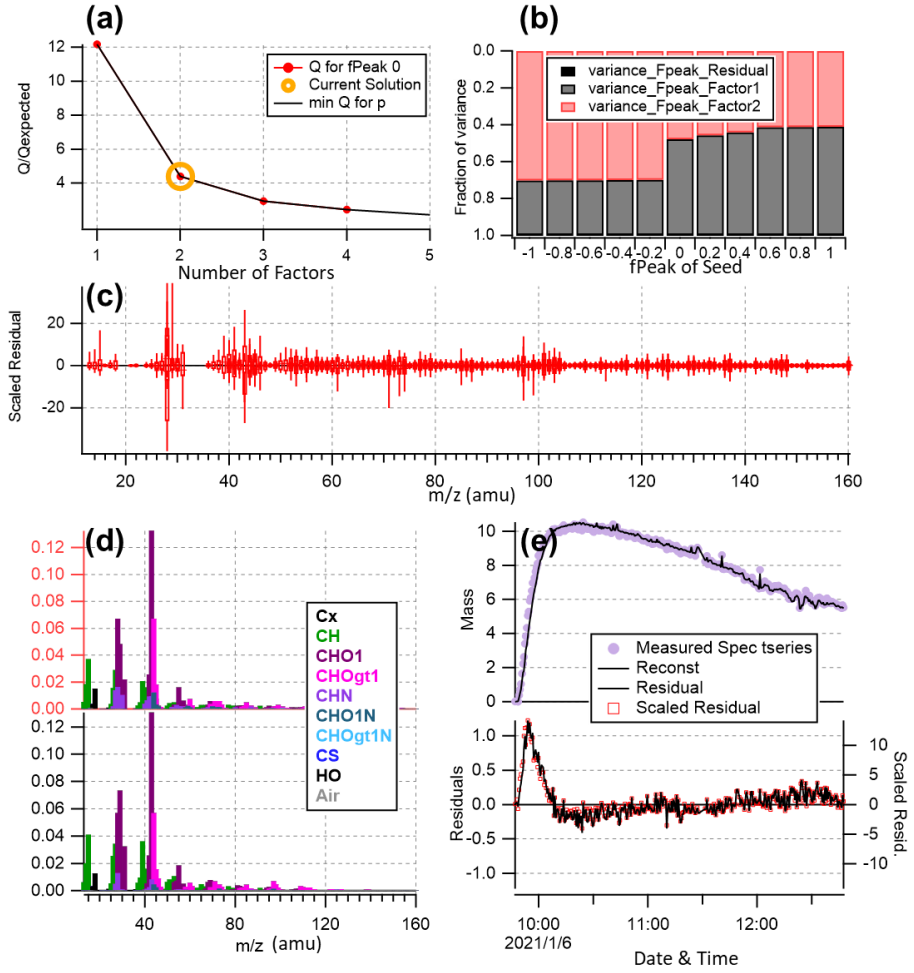


Fig. S4 The 2-factor solution for the toluene OH-oxidation in the presence of $NH_3$.

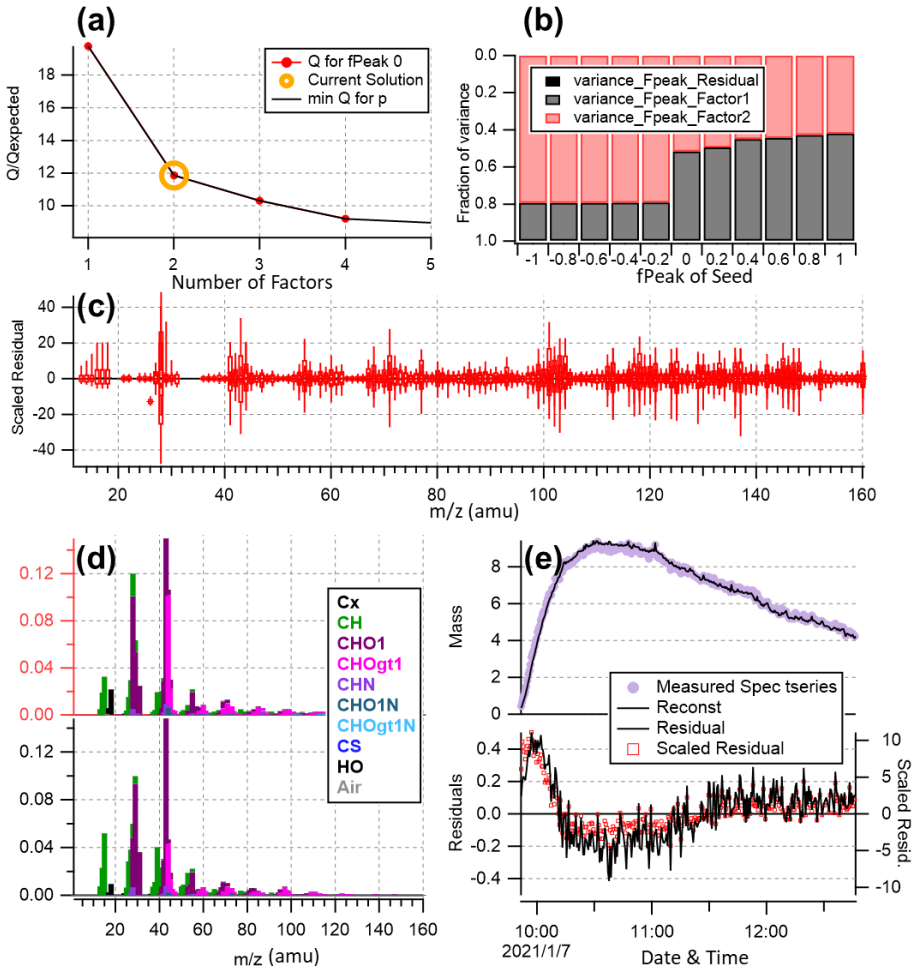


Fig. S5 The 2-factor solution for the toluene OH-oxidation in the presence of NOx.

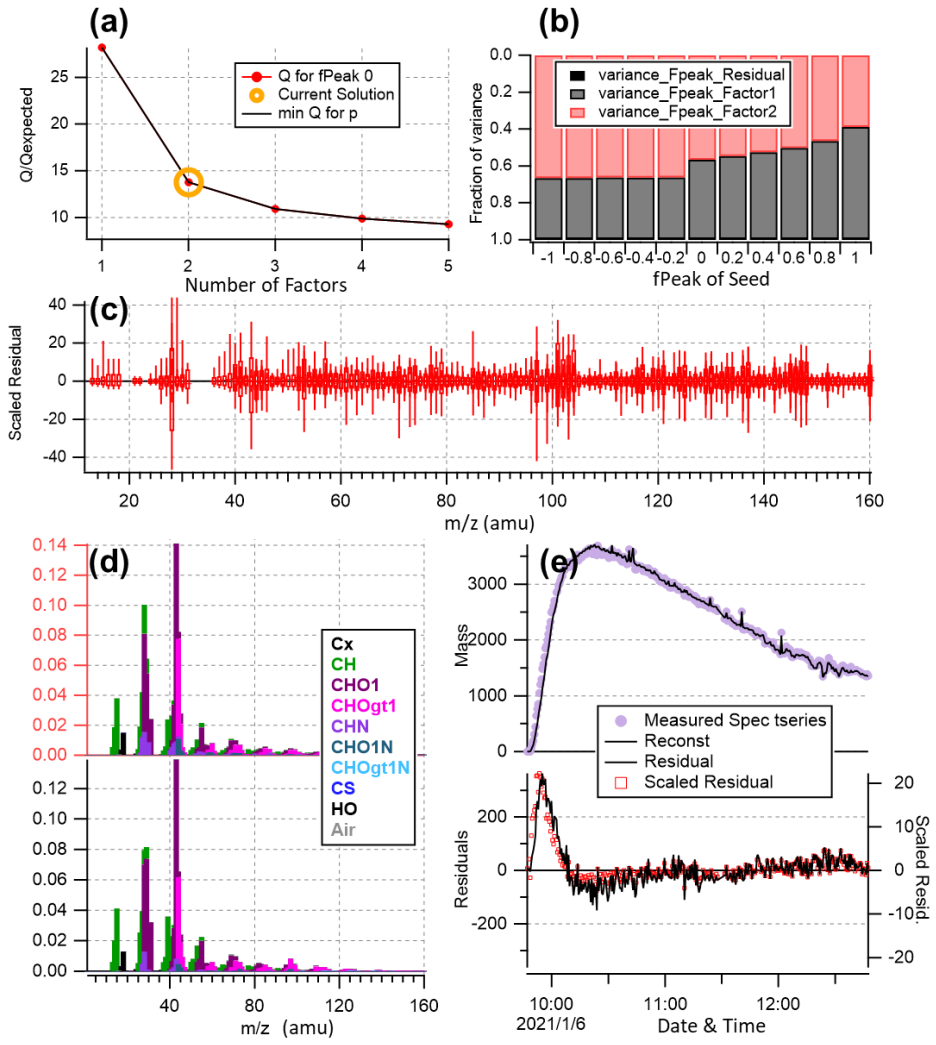


Fig. S6 The 2-factor solution for the toluene OH-oxidation in the presence of both NOx and $NH_3$.

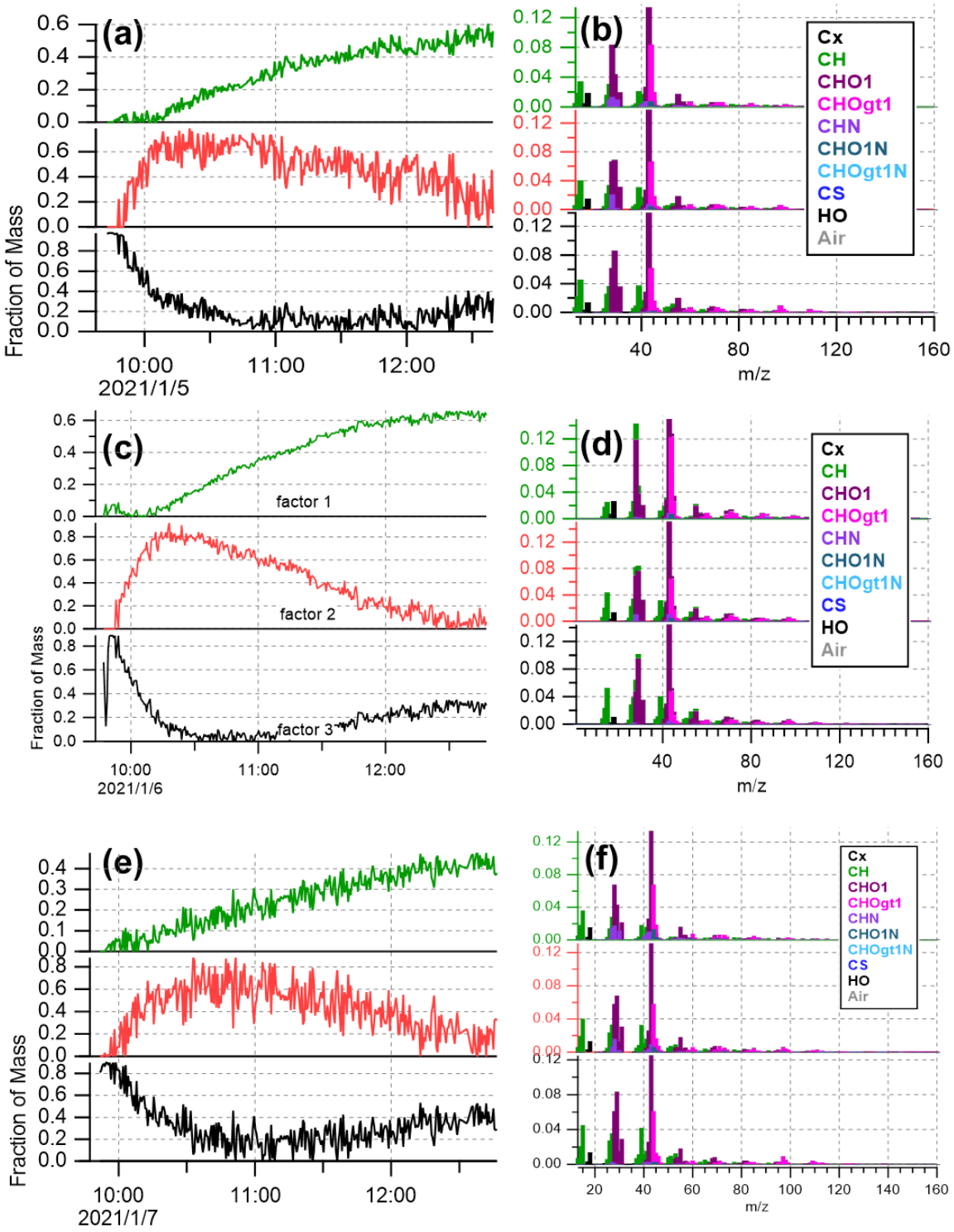


Fig. S7 (a), (c), and (e): Time series of mass concentration of OA in each factor. (b), (d), and (f): High resolution mass spectra 3-factor solution for the Exp. 2, 3, and 4, respectively.

## Reference:


Chen, T. Z., Liu, Y. C., Ma, Q. X., Chu, B. W., Zhang, P., Liu, C. G., Liu, J., and He, H.: Significant source of secondary aerosol: formation from gasoline evaporative emissions in the presence of $SO_2$ and $NH_3$, Atmos. Chem. Phys., 19, 8063-8081, 10.5194/acp-19-8063-2019, 2019.

Chen, T. Z., Chu, B. W., Ma, Q. X., Zhang, P., Liu, J., and He, H.: Effect of relative humidity on SOA formation from aromatic hydrocarbons: Implications from the evolution of gas- and particle-phase species, Sci. Total. Environ., 773, 145015, 10.1016/j.scitotenv.2021.145015, 2021.

Chhabra, P. S., Ng, N. L., Canagaratna, M. R., Corrigan, A. L., Russell, L. M., Worsnop, D. R., Flagan, R. C., and Seinfeld, J. H.: Elemental composition and oxidation of chamber organic aerosol, Atmos. Chem. Phys., 11, 8827-8845, 10.5194/acp-11-8827-2011, 2011.

Docherty, K. S., Corse, E. W., Jaoui, M., Offenberg, J. H., Kleindienst, T. E., Krug, J. D., Riedel, T. P., and Lewandowski, M.: Trends in the oxidation and relative volatility of chamber-generated secondary organic aerosol, Aerosol Sci. Technol., 52, 992-1004, 10.1080/02786826.2018.1500014, 2018.

Kroll, J. H., Donahue, N. M., Jimenez, J. L., Kessler, S. H., Canagaratna, M. R., Wilson, K. R., Altieri, K. E., Mazzoleni, L. R., Wozniak, A. S., Bluhm, H., Mysak, E. R., Smith, J. D., Kolb, C. E., and Worsnop, D. R.: Carbon oxidation state as a metric for describing the chemistry of atmospheric organic aerosol, Nat. Chem., 3, 133-139, 10.1038/nchem.948, 2011.

Liu, T. Y., Wang, X. M., Deng, W., Zhang, Y. L., Chu, B. W., Ding, X., Hu, Q. H., He, H., and Hao, J. M.: Role of ammonia in forming secondary aerosols from gasoline vehicle exhaust, Sci. China Chem., 58, 1377-1384, 10.1007/s11426-015-5414-x, 2015.

Liu, Y. C., Li, S. M., and Liggio, J.: Technical Note: Application of positive matrix factor analysis in heterogeneous kinetics studies utilizing the mixed-phase relative rates technique, Atmos. Chem. Phys., 14, 9201-9211, 10.5194/acp-14-9201-2014, 2014.

Paatero, P., and Tapper, U.: Positive matrix factorization: A non-negative factor model with optimal utilization of error estimates of data values, Environmetrics, 5, 111-126, 10.1002/env.3170050203, 1994.

Paatero, P.: Least squares formulation of robust non-negative factor analysis, Chemometr. Intell. Lab., 37, 23-35, Doi 10.1016/S0169-7439(96)00044-5, 1997.

Paatero, P., Hopke, P. K., Song, X. H., and Ramadan, Z.: Understanding and controlling rotations in factor analytic models, Chemometr. Intell. Lab., 60, 253-264, Doi 10.1016/S0169-7439(01)00200-3, 2002.

Park, J. H., Babar, Z. B., Baek, S. J., Kim, H. S., and Lim, H. J.: Effects of NOx on the molecular composition of secondary organic aerosol formed by the ozonolysis and photooxidation of α-pinene, Atmos. Environ., 166, 263-275, 10.1016/j.atmosenv.2017.07.022, 2017.

Ruggeri, G., Bernhard, F. A., Henderson, B. H., and Takahama, S.: Model-measurement comparison of functional group abundance in α-pinene and 1,3,5-trimethylbenzene secondary organic aerosol formation, Atmos. Chem. Phys., 16, 8729-8747, 10.5194/acp-16-8729-2016, 2016.

Ulbrich, I. M., Canagaratna, M. R., Zhang, Q., Worsnop, D. R., and Jimenez, J. L.: Interpretation of organic components from Positive Matrix Factorization of aerosol mass spectrometric data, Atmos. Chem. Phys., 9, 2891-2918, 10.5194/acp-9-2891-2009, 2009.